Molecular Crystals and Liquid Crystals Incorporating Nonlinear Optics

Publication details, including instructions for authors and subscription information:
http://www.tandfonline.com/loi/gmcl17

Electric Field Induced Texture Transitions in the Planar Smectic A Phase of Some Cyanobiphenyls

D. K. Rout [a] & R. N. P. Choudhary [a]

[a] Department of Physics & Meteorology, Indian Institute of Technology, Kharagpur, 721302, India

Version of record first published: 22 Sep 2006.

To cite this article: D. K. Rout & R. N. P. Choudhary (1989): Electric Field Induced Texture Transitions in the Planar Smectic A Phase of Some Cyanobiphenyls, Molecular Crystals and Liquid Crystals Incorporating Nonlinear Optics, 166:1, 75-90

To link to this article: http://dx.doi.org/10.1080/00268948908037139

Mol. Cryst. Liq. Cryst., 1989, Vol. 166, pp. 75–90
Reprints available directly from the publisher
Photocopying permitted by license only

Printed in the United States of America

Electric Field Induced Texture Transitions in the Planar Smectic A Phase of Some Cyanobiphenyls

D. K. ROUT and R. N. P. CHOUDHARY

Department of Physics & Meteorology, Indian Institute of Technology, Kharagpur 721302, India

(*Received December 22, 1987; in final form April 6, 1988*)

Observations of zero field textures and electric field induced defects in the planar smectic A of the cyanobiphenyl group of liquid crystals are presented. Two transitions, first from the parabolic focal conic texture to a texture consisting of array line defects and then to a quasi-homeotropic texture are observed under the influence of an electric field. The line defects are interpreted as edge dislocations. The current-voltage characteristics and the electro-optic studies confirm the existence of the above two transitions. A long optical memory effect is realised from the electro-optic studies. A decrease in the current density is associated with the transition to the memory state.

INTRODUCTION

The smectic A (SmA) may be described as a stack of two dimensional liquid layers, which can easily be curved and flow over one another, keeping the interlayer thickness constant. The rod like molecules in the SmA have their long axes oriented normal to the layers. This makes the system optically uniaxial, with a large optical anisotropy. The textures formed in this phase depend on a number of factors such as (a) surface conditions of the glass plates used, (b) nature of interaction of the molecules with the surfactants, (c) cell thickness, (d) temperature, etc. Friedel and Grandjean[1] showed that planar SmA textures occur in focal conics. The smectic layers in the focal conic textures are supposed to be arranged in Dupin cyclides and the most striking defect in this structure should be ellipses and hyperbolae in a confocal relationship. Bouligand,[2] however, proved that the curves may be conics, but not in a precise focal conic relationship. Rosenblatt *et al.*[3] have shown that the focal conic defects in a planar SmA sample are essentially pairs of confocal parabolae (parabolic focal conic).

Some work has been reported earlier on the effects of electric and magnetic fields on the SmA phase. The electrical analogue of Frederiks transition in the SmA phase was studied theoretically by Rapini[4] and experimentally by Goscianski *et al.*[5] Their studies show that the Frederiks transition in SmA is not detectable optically as a very small change in the molecular orientation takes place and the

transition has been termed a ghost transition. The texture transitions in the SmA phase under an electric field were first studied by Tani.[6] But the mechanism of such transitions was not clear then. Hareng *et al.*[7] studied the field induced texture transition in a high quality planar texture of the SmA phase of octylcyanobiphenyl. Their observation revealed that under the influence of a strong electric field, a SmA planar sample with large positive dielectric anisotropy ($\Delta\epsilon$) undergoes transition from a planar to a quasi-homeotropic texture. But virtually no analysis was made on the nature of the defects. Recently Aliev and Mamedov[8] observed vortical EHD instability in the SmA phase of a ternary liquid crystal mixture as well as in 4-cyanobenzylidene-4-*n*-octylaniline (CBOA). They have shown that artificial creation of certain changes in the electrical conductivity of the substance is the necessary criterion for the occurrence of such types of instability.

A scattering texture in SmA could be obtained[9] when a homeotropic nematic sample of positive $\Delta\epsilon$(8CB) was cooled down to the SmA phase under an alternating electric field. In the case of planar samples, the light scattering structure could also be obtained under a sufficiently high field which has a long optical memory effect.[10] But in all cases, no detailed understanding of the phenomena was made.

In the present paper, we first discuss the planar texture of the SmA phase of the cyanobiphenyl group of liquid crystals. When the well-aligned SmA structure was subjected to an electric field, a series of phenomena occurred. In the process, observed electrohydrodynamic (EHD) instability patterns in the compounds are discussed. The electro-optic properties have also been studied in order to examine their relation with the electrical conduction of the materials. An attempt has been made to understand the mechanism of texture changes under the electric field.

2. EXPERIMENTAL

The following four compounds having positive $\Delta\epsilon$ have been used in the present study and the mesophase transitions of the compounds are shown along with them:

4′-*n*-octyl-4 cyanobiphenyl (8CB)
K 21.5°C SmA 33.5°C N 40.5°I
4′-*n*-octyloxy-4-cyanobiphenyl (8OCB)
K 54.5°C SmA 67°C N 80°C I
4′-*n*-nonyl-4-cyanobiphenyl (9CB)
K 42°C SmA 48°C N 49.5°C I
4-*n*-nonyloxy-4-cyanobiphenyl (9OCB)
K 64°C SmA 77.5°C N 80°C I

The compounds were obtained from M/s BDH Ltd., England and were used without further purification. The transition temperatures were found to be the same as the above reported values.[11] For microscopic as well as electrical measurements, the samples were sandwiched between two SnO_2-coated glass plates with mylar spacers of 50 μm thickness. To obtain the planar arrangement (molecular

long axes parallel to glass slides), the cleaned glass plates were treated with polyvinyl alcohol and then rubbed unidirectionally. Excellent planar samples were obtained after cooling down the samples slowly (~1° C/min) from the isotropic state. The textures of the compounds in different conditions in the SmA phase were studied under a Censico Polarising microscope with microphotographic equipment. The temperature was maintained with accuracy better than 1°C in the hot stage, fabricated by us (described elsewhere)[12] with the help of an Indotherm temperature controller.

DC voltage (0-100V) was applied to the sample cell with an Aplab power supply and the current flow through the cell was measured with the help of a DC nanoammeter.

The electro-optic properties were studied with the help of a photodiode fitted to the eyepiece of the microscope. A 5 mw He-Ne laser (Spectra-Physics) was used as the monochromatic source of light. The recording of transmitted light intensity was performed with the help of a digital memoryscope (Iwatsu DMS-6430) at a clockrate of 10 μs per WD and a data length of 1024 WD.

3. MICROSCOPIC OBSERVATIONS

3.1. Zerofield texture of the planar SmA phase

Various types of focal conic textures have been observed[3,13] in the SmA phase. The textures have been classified into four different combinations[14]: (a) cylindrical-straight line, (b) toric-domains, (c) ellipse-hyperbola in confocal positions (normal focal conic domain) and (d) two parabolae in confocal positions (parabolic focal conics, (PFC)).

Three different types of textures were obtained in planar samples of the present compounds depending upon the rate of cooling from the isotropic state. Fan shaped textures were obtained when the cooling rate was fast. A mixture of normal focal conic domains and PFCs were obtained when the cooling rate was medium. (~2° C/min). When the cooling rate was very slow (~0.5°C/min), a pure parabolic focal conic texture was obtained which is shown in Figures 1a,b,c. The parabolae become narrower and narrower if the cooling rate becomes sufficiently slow, provided, of course, that the surface conditions are uniform. PFCs were found to be similar in appearance in all four compounds. Some of the unique features observed in the PFCs are given as follows:

(a) The appearance is described as a parabola with a tail (a straight line). Both appeared as dark lines when the analyser and polariser were inclined at 60° [Figure 1b]. Under crossed polarisers the parabolae appeared in white lines [Figure 1a]. The observed parabolae and the straight lines are conic sections in perpendicular planes, one going through the focus of the other. The straight line is actually the orthogonal parabola of the one that is visible.

(b) The PFCs are not necessarily lie in the plane of the glass slides. In fact, we have observed a tilt in the Figures 1a,b.

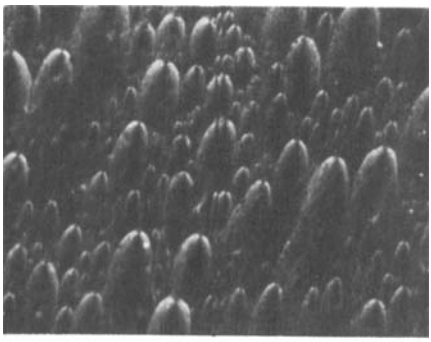

(a)

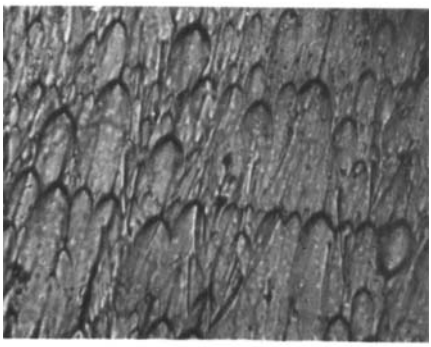

(b)

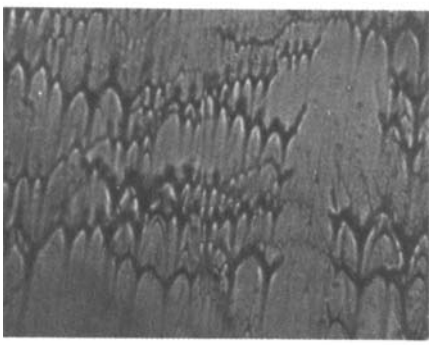

(c)

FIGURE 1 The parabolic focal conic (PFC) texture of planar SmA phase of 8CB (25°C) (a) crossed polarisers (b) analyser and polarisers inclined at 60° (c) showing antiparallel arrangement at both glass surfaces ($\times 450$).

(c) An antiparallel arrangement of the PFCs was observed at the opposite glass surfaces. While changing the focus of the microscope, this is clearly observable (Figure 1c).

(d) The size of the parabolae depends on the surface preparations. Due to different surface anchoring conditions, the size of the parabolae is not uniform throughout the observed area of the sample.

During our experiments, we have also observed the focal conic textures of the above classification (b) *i.e.*, the toric domains [Figure 2a]. It is actually a rare defect texture. At this stage, it is not known whether this defect appeared under the influence of the electric field! The dark lines are the defects created under an electric field, which will be discussed in the following sections. However, these defects are found to be isolated defects.

3.2. Electric field induced textures

The defect textures under an electric field depend on their initial zero field structure. The texture changes of all four samples are similar. The differences (if any) are only due to the initial difference in the zero field texture and the temperature of the mesophase.

The basic features of the formation of the defects under an electric field common to all the samples are as follows:

(a) Visible oscillation of the PFCs in the plane of the glass slides are observed just prior to the threshold field for instability.

(b) At the threshold voltage, the PFCs lie side by side, thereby forming a fringe pattern [Fig. 2b]. The lines then start to appear just after the threshold voltage, V_{TH}. A closer and careful inspection along the lines reveal that the PFCs are lying antiparallel on both the sides of the line defects [Figures 2c, 2d]. Clear wavy lines are also formed at some places [Figure 2d]. With the increase of the applied voltage, the lines grow along one direction in the plane of the glass plates. However, we have not observed any preferred direction of the growth of the defects. At higher voltages, (viz. $\sim$ 60 V for 9 CB), an array of line defects are formed. This array of lines is not necessarily periodic (Figure 2e).

The formation of the fringes in the cell is the preparatory stage for the occurrence of the instability. With the increase of the applied voltage, the instability is suppressed and the array of line defects is formed. The line defects are also visible with or without crossed polarisers. It seems that these linear defects are edge dislocations.

A closer inspection of the array of line defects [Figure 2f] shows that the parabolae of the PFCs transform to ellipses or circles along the line defect and lie antiparallel to each other. This observation seems to suggest that at higher fields, the dipole moments, which are along the molecular long axes for the present compounds, try to align themselves along the direction of the applied field. As a result, there is a bend in the layer structure, keeping the inter-layer distance intact [Figure 3a]. The edge dislocations arising out of the above bending result in the appearance of dark lines. With the subsequent increase of the applied field, a clustering of edge dis-

FIGURE 2a The defect texture showing the line defects at 30 V for 8CB as well as the rare toric domains (No analyser, ×225).

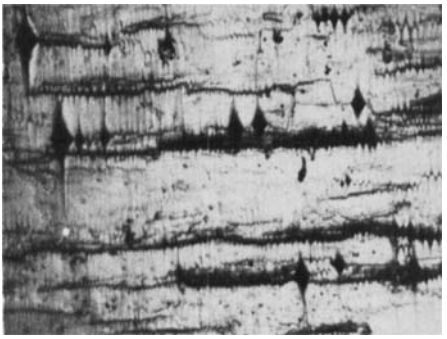

FIGURE 2b Fringe pattern at 30 V for 8CB (25°C), (crossed polars ×450).

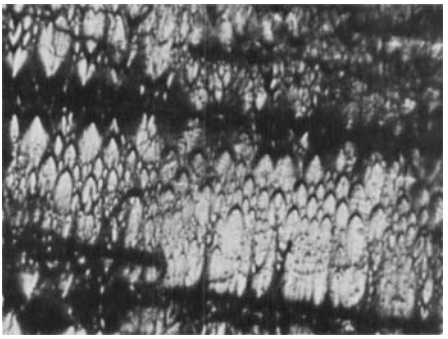

FIGURE 2c Line defects (dislocations) at 55 V for 8CB (25°C), showing antiparallel arrangement of PFCs along the line defect (×450).

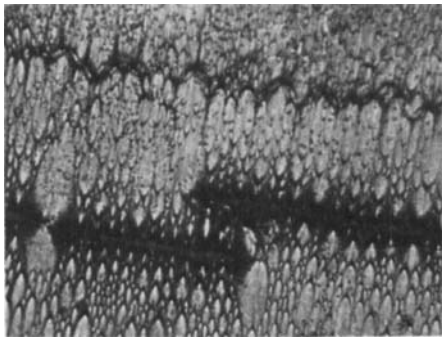

FIGURE 2d Line defects as well as wave patterns at 44 V for 9CB (44°C) (×450).

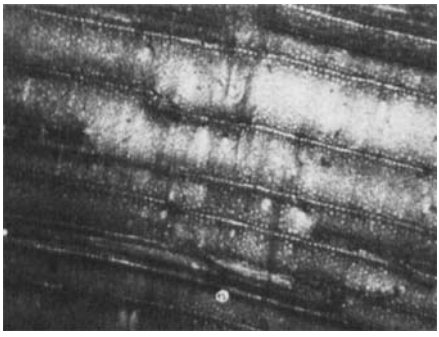

FIGURE 2e Array of line defects at 60 V for 9CB (44°C) (×225).

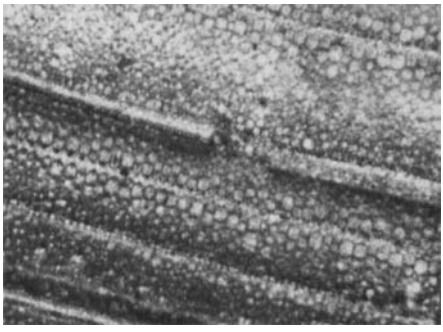

FIGURE 2f Same as Figure 2e at higher magnification (×450) showing the PFCs having turned to circles.

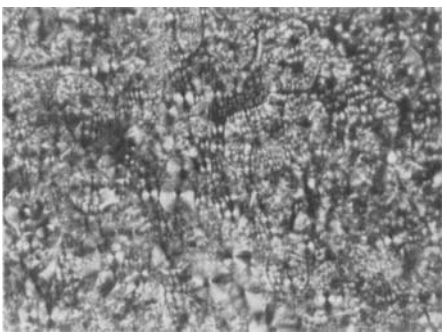

FIGURE 2g Concentric rings at some singular points (at 50 V for 8CB at (T_{SN-1})°C (T_{SN}: Temperature at which transition from smectic to nematic phase takes place).

locations may be formed at the site of unit dislocation, resulting in very thick dark lines [Figure 2c].

If the applied field is increased even after the formation of the array of defects, the earlier surface anchoring conditions are destroyed and hence the PFC structure is nowhere visible. From the distorted planar orientation, it now transforms to a quasi-homeotropic orientation. As expected, the transition is rather slow. This type of transition occurs at ~50 V for 8CB at (T_{SN} − 1°C). The texture appears as concentric rings around some singular points (Figure 2g). This structure is typical of homeotropic alignment.[5] The concentric ring structure has been interpreted as stable grain boundaries in the presence of an applied electric field.

One important observation is that the defects created under the electric field (array of line defects) are irreversible. This irreversible phenomena is possible due to the fact that the surface anchoring energy is not sufficient to counter the dislocations created under the electric field. Only a higher energy (*i.e.* thermal energy, required to go to the nematic phase) destroys the defects.

Unlike many other defects, observed in liquid crystals, the dislocations occur in the middle of the sample, whereas the planar orientation remains intact at the glass surface. Actually, the PFCs and the line defects are coexisting, which can be seen in Figure 2d. The defect texture can stay together for days without any visible change. As observed earlier[6,9] the defect texture can only be erased after heating it to the nematic phase.

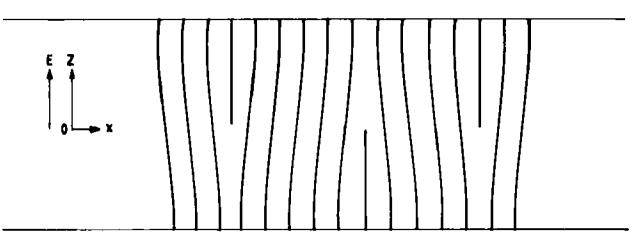

FIGURE 3 Formation of dislocations in a planar smectic subjected to intense electric field.

4. J-V CHARACTERISTICS UNDER DC FIELD

J-V characteristics of liquid crystals, in general, reflect the nature of the instability which occurs in the nematic and smectic phases. Aliev and Mamedov[8] showed that a non-uniform distribution of the electrical conductivity over the specimen is responsible for the regular vortical EHD instability in the SmA liquid crystals. Moreover, a close relation between the carrier mobility and the electro-optic properties of the SmA liquid crystals has been shown by Yoshino *et al.*[15]

Figures 4a, b, c, d show the J-V characteristics of the samples 8CB, 8OCB, 9CB and 9OCB respectively. The most important observation worth noting regarding the J-V characteristics of all the samples is the increase of resistance of the sample above the threshold voltage. After a few volts, the current values increase again. The threshold voltage and the plateau region depend upon the temperature. The plateau becomes flatter with the decrease of temperature. Even at lower temperatures (near the crystalline-SmA phase) the phenomena of increasing resistance does not occur and also the plateau is not prominent. In the case of the 9CB sample, we have not observed the above phenomena except very feebly at 46°C. That is due to the fact that the 9CB sample used in the present experiment is not a virgin one. It has been observed by us that while decreasing the voltage, the above phenomena of increasing resistance and plateau do not exist. These types of observations have also been observed by Yoshino *et al.* in the CBOA sample.

The above observations confirm our earlier microscopic observations that an EHD instability starts just below the threshold voltage where the current values are increasing steeply. After the threshold voltage, the instability is suppressed and a rather stable defect structure is formed. The increase in the resistance values is a result of a transformation from the high mobility to the low mobility state. In the low mobility state, the carriers are quite rigid because of the creation of the defects. Again the increase in the current values coincides with the transformation of the defect state to the homeotropic state. In the homeotropic state, the conductivity value is normally higher than the planar alignment for the present compounds. The voltages at which the above mentioned two transitions *i.e.* (i) high mobility to low mobility state (Tr. 1) and then (ii) low mobility to homeotropic state (Tr. 2) take place, vary from compound to compound as well as with the temperature.

Although it is very difficult to strictly compare the above observed properties in the context of the molecular structure of the compounds, an attempt has been made to compare the four compounds in the context of the above observed results.

(a) V_{Tr1}, V_{Tr2} (the voltages at which Tr1 and Tr2 take place respectively) decrease with increasing temperature for all four compounds.

(b) The plateau becomes narrower with increasing temperature.

(c) However, we could not observe any systematic relation between the V_{Tr1}, V_{Tr2} and the molecular structure of the compounds. V_{Tr} values for 9OCB are the highest of all. These observations suggest that the surface conditions and the zerofield alignment are more responsible than the molecular structure of the compounds.

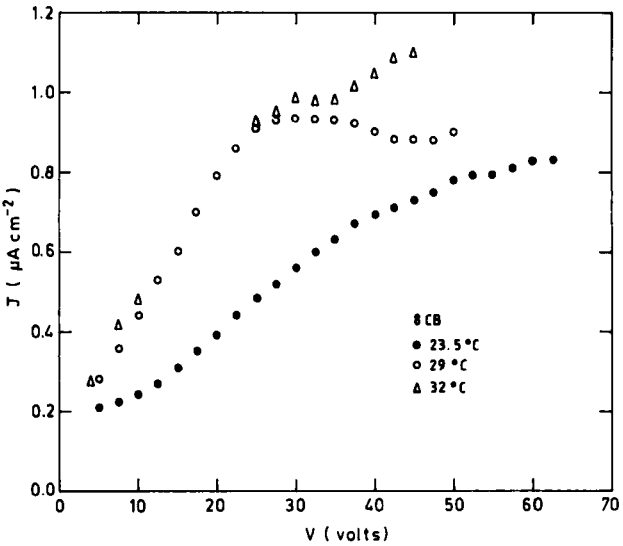

FIGURE 4a J-V characteristics at different temperatures for 8CB.

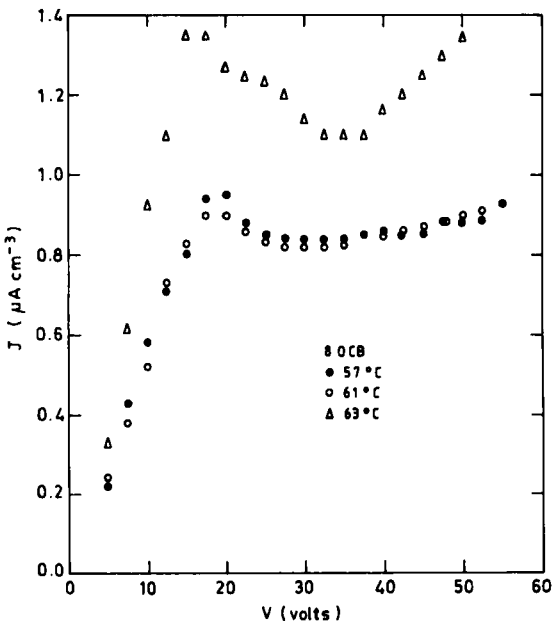

FIGURE 4b J-V characteristics at different temperatures for 8OCB.

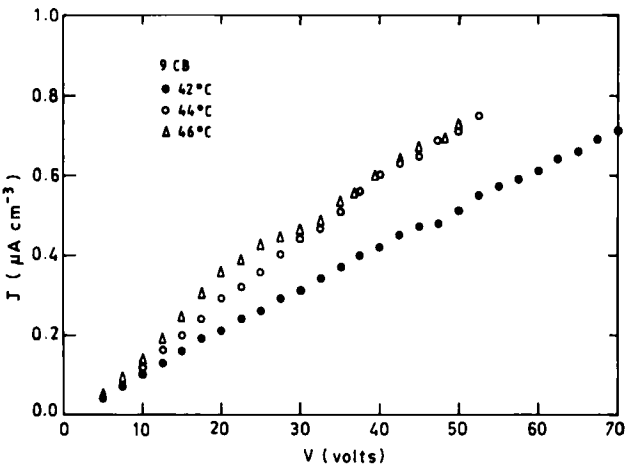

FIGURE 4c J-V characteristics at different temperatures for 9CB.

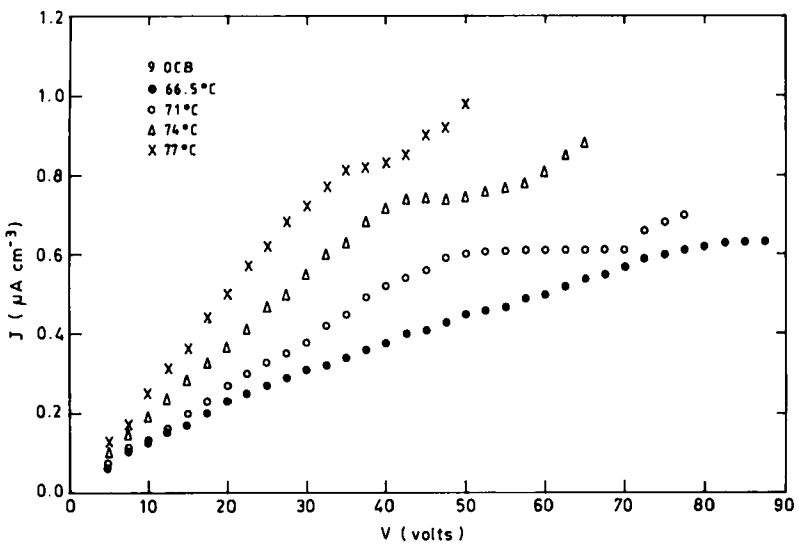

FIGURE 4d J-V characteristics at different temperatures for 9OCB.

Figure 5 shows the dc conductivity of the 8CB and 9CB samples before and after an electric field was applied. It has been observed that in the case of 8CB, there is a larger difference between the conductivity of the virgin sample and the sample to which 90 V was applied. Less difference in the conductivity is observed between the virgin sample of 9CB and the sample to which 100 V was applied. When the sample was heated to the nematic phase, there is no difference in the conductivity between the virgin sample and the sample to which high voltage was applied. It

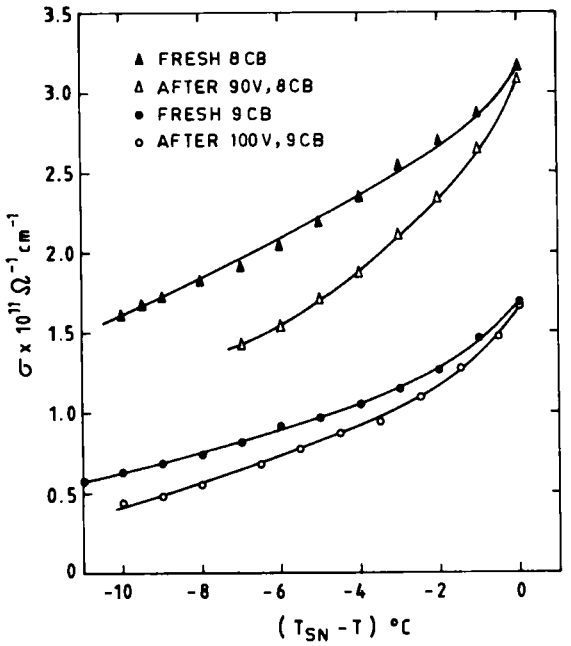

FIGURE 5 Variation of d.c. conductivity with temperature.

indicates the fact that, heating to the nematic phase, previous defects created under an electric field in the smectic phase can be erased.

5. ELECTRO-OPTIC EFFECTS

The electro-optic effects in the liquid crystals[16,17] are considered to have close relations with the mechanisms of the electrical conduction in these materials. The application of a large voltage (100 V) to a thin layer of smectic A produces changes in its optical properties in surprisingly short time (10 to 100 m sec). The effects can be divided into those based on scattering which seem to have its origin in hydrodynamic motion and those based on a reorientation induced by dielectric torques. These electro-optic effects often show memory[6] and can be erased electrically; they therefore offer attractive possibilities for use in multiplexed displays. In most cases, no detailed understandings of the phenomena exists. Here we have attempted to study the relation between the electro-optic effects and the electrical conductivity of the SmA phase of the present compounds. The light transmission under an applied electric field has been studied at various temperatures for the 8CB, 9CB, 8OCB and 9OCB samples and are shown in Figures 6a, b, c, d respectively.

The main characteristics of the transmitted intensity versus applied voltage for all four samples are:

(a) There is a close relationship between the J-V characteristics and the above electro-optic properties.

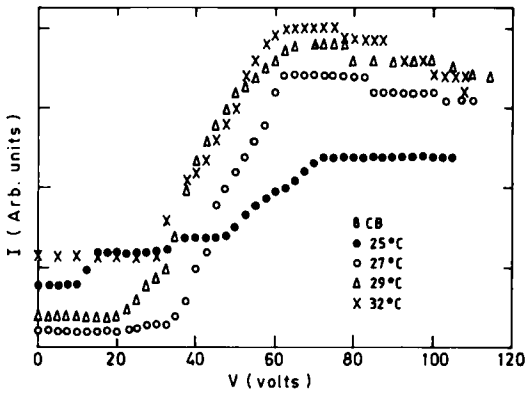

FIGURE 6a Variation of transmitted intensity with applied voltage for 8CB at different temperatures.

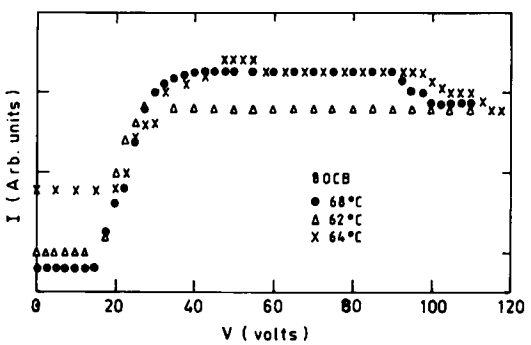

FIGURE 6b Variation of transmitted intensity with applied voltage for 8OCB at different temperatures.

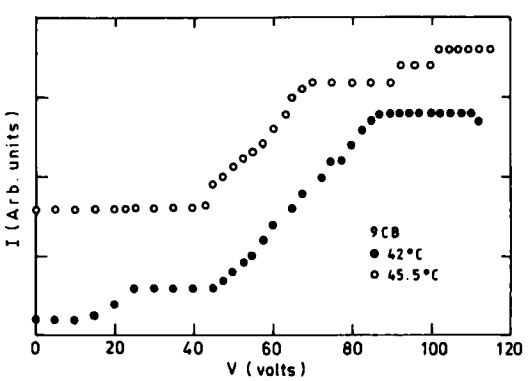

FIGURE 6c Variation of transmitted intensity with applied voltage for 9CB at different temperatures.

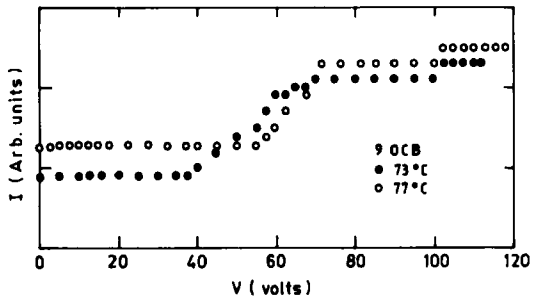

FIGURE 6d Variation of transmitted intensity with applied voltage for 9OCB at different temperatures.

(b) The transmitted intensity increases at threshold voltage, which is exactly the same voltage for Tr1 of the preceding section.

(c) The transmitted intensity keeps increasing and then remains constant. This transition corresponds to the Tr2 of the J-V characteristics.

(d) Light transmission in the low mobility state is higher than the transmission in the high mobility state.

Here, the transmission keeps increasing with decreasing conductivity and then remains constant for a fairly wide voltage, before decreasing again at very high voltage (~100 V). This decrease at high voltages is due to the occurrence of the scattering of light by the orientation of the molecules from planar to homeotropic.

When the applied voltage is removed, the defect structure still remains as mentioned earlier and hence, the transmitted intensity is also the highest, *i.e.*, it does not decrease with the withdrawal of the applied voltage. Since the transition from a lower mobility state to a higher mobility state is difficult, it takes considerable time. However, we did not observe any change in the transmitted intensity even after several days of removal of applied voltage, which indicates the defect structure to be very stable.

6. ENERGY OF THE DEFECT TEXTURES

The energy associated with the PFCs under zero field has been shown by Kléman[18] as

$$E \sim \frac{\pi k_{11}}{8} f \left(\frac{R}{f}\right)^4 \ln\left(\frac{R^2}{4fr_c}\right) \text{ for } R >> f \tag{1}$$

where, k_{11}, f, r_c and R are the splay elastic constant, focal length of the parabola, core-radius and the sample radius respectively. The energy increases with R and diverges as $f \to 0$ (R/f is constant). Thus, in general, such structures should not be energetically favourable. However, it turns out that when $R \lesssim 3f$, they can have

smaller energies and are relevant to our experimental observations. Our experimental observations show the value of f to be 4 μm. Depending upon the cooling rate, R and f values vary, but R/f remains constant. The calculated values of E for $R = 3f$, $r_c \sim 30$ Å, $k_{11} \sim 10^{-6}$ dyne was found to be $\sim 2 \times 10^{-7}$ erg.

The energy for the creation of a single dislocation under an electric field can be written as

$$E = \langle E_k \rangle + \langle E_{el} \rangle \tag{2}$$

where $\langle E_k \rangle$ is the elastic part of the energy and is generally of the form $\sim k_{11} b^2 / 2 r_c$, where b is the Buerger's vector of the dislocation and $\lambda = (k_{11}/B)^{1/2}$, where B is the layer compression modulus of the smectic layers. $\langle E_{el} \rangle$ is found to be[5] of the form $\Delta\epsilon / 16\pi$. $V_{TH}^2 / t \cdot d \sin^2\theta$ where V_{TH} is the threshold voltage (V_{Tr1}) and t is the sample thickness and d is the period of the array of defects. The values of $\langle E_{el} \rangle$ and $\langle E_k \rangle$ are of the order of $10^{-5} - 10^{-6}$ and 10^{-6} dyne respectively.

Now comparing the energies associated with various phenomena, we found that the energy associated with the PFCs is only an order lower than the energies of the defects. In fact the microscopic observations show the coexistence of the PFCs with the line defects, indicating the small difference in their energetics. Only at Tr2 the PFCs are no longer present, indicating the fact that fairly higher energy is required to destroy the PFC structure. The calculations by Hinov *et al.*[19] also show that the formation of grain boundaries (accompanying the bending of the layers) requires a surface energy in the range of 4×10^{-2} erg cm^{-2}.

7. CONCLUSIONS

1. The formation of PFCs requires less energy than the formation of normal parabolic domains. The PFCs have two parabolas crossing each other orthogonally. There is no easy or unique orientation of the PFCs, but an antiparallel arrangement at both surfaces is frequently observed. Various types of defects, even some of which (toric domains) are energetically not favourable (theoretically proved), are observed in the present investigations.

2. Two transitions have been generally observed for all four compounds. However, at lower temperatures, where the viscosity of the sample is very high, the two mobility states are not very distinct.

3. We believe that the line defects are the edge dislocations, created under the electric field, and occur at the middle of the sample. The energy of the dislocation per unit length is also of the order of 10^{-5} erg cm^{-1}.

Acknowledgments

We are grateful to M/s B.D.H. Ltd., U.K. for supplying the liquid crystals used in this study. DKR is grateful to the C.S.I.R., New Delhi for a research fellowship. We thank Dr. G. D. Nigam and Prof. K. V. Rao for their encouragement.

References

1. G. Friedel, F. Grandjean, *Bull. Soc. France Miner.*, **33**, 192 and 469 (1910).
2. Y. Bouligand, *J. de Physique*, **33**, 525 (1972).
3. Ch. S. Rosenblatt, R. Pindak, N. A. Clark and R. B. Meyer, *J. de Physique*, **38**, 1105 (1977).
4. A. Rapini, *J. de Physique*, **33**, 237 (1976).
5. M. Goscianski, L. Leger and A. Mircea-Roussel, *J. de Physique Lett.*, **36**, L313 (1975).
6. C. Tani, *Appl. Phys. Lett.*, **19**, 241 (1971).
7. M. Hareng, S. LeBerre and J. J. Metzger, *Appl. Phys. Lett.*, **27**, 575 (1975).
8. D. F. Aliev, M. M. Mamedov, *Sov. Phys. Cryst.*, **30(5)**, 553 (1985).
9. M. Hareng and S. LeBerre, *Electron. Lett.*, 11, **4**, 73 (1975).
10. L. M. Blinov in Electro-optical and Magneto-optical properties of Liquid Crystals, Wiley International (1983).
11. As per data given by M/s BDH Ltd., UK.
12. D. K. Rout and R. N. P. Choudhary, *Mol. Cryst. Liq. Cryst.*, **154**, 241 (1988).
13. D. Demus and L. Richter, *Textures of Liquid Crystals*, Verlag Chemie (1978).
14. S. Chandrasekhar and G. S. Ranganath, *Adv. Phys.*, **35**, 507 (1986).
15. K. Yoshino, K. Yamashiro and Y. Inuishi, *Jpn. J. Appl. Phys. 14*, **2**, 216 (1975).
16. G. H. Heilmeier and J. E. Goldmacher, *Appl. Phys. Lett.*, **13**, 132 (1968).
17. W. Helfrich, *J. Chem. Phys.*, **51**, 4092 (1969).
18. M. Kléman, *J. de Physique*, **38**, 1511 (1977).
19. H. P. Hinov, N. Shonova and K. Avramova, *Mol. Cryst. Liq. Cryst.*, **97**, 297 (1983).